



Assessment of a Slope Stability Using the Classical and Modified Circular Cylindrical Sliding Surface Methods

Amandyk Tuleshov, Bagdat Teltayev* and Aizhan Muta*

Abstract

In this work, the stability of the slope of Mount Kok Tobe is assessed under the following three conditions: condition 1 - the soil of the slope is homogeneous and is completely in its natural state; condition 2 - the surface layer of the slope 70 cm thick is moistened by rainwater and it is assumed that the sliding surfaces are deep (below the base of the slope); condition 3 - the surface layer 70 cm thick is moistened by rainwater and it is assumed that the sliding surfaces are close to the moistened surface layer of the slope. The assessment of slope stability was carried out using the circular cylindrical sliding surface (CCSS) method. A modified CCSS method has also been developed and used in the calculations, which, together with the Terzaghi-Fellenius method, makes it possible to speed up and increase the accuracy of determining the position and characteristics of sliding surfaces. It is established that the slope has an insignificant margin of stability. To increase the stability of the slope, it is recommended to sow apple trees of the apor variety, which coincide in existence and fertility with the conditions of Kok Tobe Mountain.

Keywords: Calculations of mountain slope stability; Circular cylindrical sliding surface method; Modified CCSS method; Atmospheric precipitations.

Received: 18 October 2025; Revised: 09 November 2025; Accepted: 10 November 2025

Article Type: Research article.

1. Introduction

Slope stability is one of the key tasks of geotechnical engineering, critical for infrastructure safety and landslide prevention. Classical assessment methods, such as the Terzaghi-Fellenius and Bishop method, make it possible to determine the stability factor and the critical sliding surface, but their application is limited by complex geometries and soil heterogeneity.^[1,2]

The method of a circular cylindrical sliding surface (CCSS)^[3] is more practically acceptable, which is more accurate and faster than the Terzaghi-Fellenius and Bishop methods.

But it should be remembered that modern more advanced methods require knowledge of a lot of specified data, for example, since the porosity of the coefficient of thermal and moisture conductivity, heat capacity, maximum capillary moisture capacity, and others. It is also necessary to know the structure of the slope, the physical and mechanical characteristics of all types of soils that make up the slope. As a rule, at the initial stage of studying slope stability, the above

characteristics are still unknown. Getting all of them requires a lot of time and material resources. With that said, at the initial stage of analyzing the problem, it is very useful to obtain primary information about the stability of the mountainside using approximate methods, one of which is the CCSS method. The results obtained with its application can serve as a basis for further in-depth research and for the urgent adoption of protective and preventive measures.

With the development of numerical methods such as FEM, Strength-Reduction FEM, and three-dimensional models using SPH, it has become possible to more accurately simulate the stress state, deformations, and progressive fracture of slopes under the influence of rainfall and surface runoff.^[4-9] Numerical methods also allow for the consideration of hydrological processes affecting slope stability, including infiltration and surface runoff during heavy rains.^[10-13]

In recent years, artificial intelligence methods and metaheuristic algorithms have been actively used, which make it possible to take into account many factors simultaneously and improve slope stability prediction.^[14-15] The analysis of geosynthetically reinforced soil structures also expands the possibilities of engineering slope design in difficult conditions.^[16] At the same time, assessing the stability of complex three-dimensional slopes and the effects of extreme

U. A. Joldasbekov Institute of Mechanics and Engineering, Almaty, 050010, Kazakhstan

*Email: bagdatbt@yahoo.com (Bagdat Teltayev),
mutita@mail.ru (Aizhan Muta)

precipitation remain urgent tasks requiring the integration of classical, numerical, and AI approaches to improve the accuracy and reliability of design solutions.^[8,10-13,17-21]

In this paper, a preliminary assessment of the stability of the slope of Kok Tobe Mountain, taking into account the moistening of the surface layer of the slope by precipitation, was carried out using classical and modified CCSS methods.

2. Almaty and Kok Tobe Mountain

Almaty is an ancient city at the foot of the Trans-Ili Alatau. The first settlements in its place existed already in the 1st millennium bc as a point of the Great Silk Road. In 1854, the Verny fortification appeared here, since 1921 the city was called Alma Ata, and in 1993 it received its modern name. Until 1997, Almaty was the capital of Kazakhstan, and today it remains the largest cultural and financial center of the country.

Modern Almaty (population as of October 2023 - 2,211,198 people) is located at an altitude of 600-900 m above sea level in the zone of foothill and mountain slopes with a sharply continental climate and an annual precipitation of 550-700 mm (Fig. S1). This area combines high seismicity, steep slopes, and intensive atmospheric precipitation, which increases the risk of landslide processes.

The foothills of Almaty are characterized by high biodiversity. They are home to the Sievers apple tree, walnut and birch groves, spruce forests above the belt, as well as rare species from the Red Book of Kazakhstan, such as the snow leopard, the Tien Shan brown bear, the Turkestan lynx, the golden eagle, the vulture, and others.^[22] The preservation of this ecosystem is of strategic importance for the sustainable development of the region. The city's symbol is the legendary Apport apple, whose optimal growing zone (850-1250 m) coincides with the conditions of the Kok Tobe mountain slopes. The new state program for 2024-2028 envisages the revival of Apport with the selection of sustainable clones,^[23] which can be combined with the biostabilization of the slopes.

Kok Tobe Mountain, located approximately 1,100 meters above sea level, is a prominent natural landmark and one of the main tourist attractions in Almaty. It is home to a television tower, a recreation park, a cable car, and observation decks. In 2022, a fire broke out on the mountain's slope, destroying approximately 3 hectares of vegetation,^[24] highlighting the vulnerability of the site to natural and man-made hazards. Given the recreational pressure and landslide processes, it is important to maintain the stability of the Kok Tobe mountain slopes, prevent erosion, fires, and soil degradation through monitoring, drainage, slope stabilization, and the preservation of local flora.

3. Landslides in the vicinity of almaty

In 2016-2024, several landslides of various scales occurred in the foothills of Almaty, near the slopes of Kok Tobe Mountain. The main cause of most of these events was the waterlogging of the soil due to atmospheric precipitation (rain, snow, and snowmelt), or man-made leaks exacerbated by anthropogenic disturbances on the slopes.

On May 11, 2016, a clay-mud landslide with a volume of about 2,000 m³ occurred in the Alatau microdistrict, partially destroying a two-story house (Fig. S2).^[25]

On May 20 of the same year, a landslide with a volume of about 25,000 m³ occurred below the Medeu ice rink, partially blocking the Kishi River in Almaty.^[26] In April 2017, two small landslides were recorded: on April 13, at the BAK Alma PC street (≈30 m³),^[27] and on April 29, near the Ainabulak sanatorium (≈50 m³),^[28] both damaged infrastructure and blocked the roadway.

Three major events were recorded in 2023 and 2024. On February 27, 2023, a ~360 m³ landslide crossed a concrete retaining wall and damaged residential buildings in the village of Besagash after mixed precipitation (Fig. S3).^[29]

On February 8, 2024, a catastrophic landslide with a volume of approximately 3,200 m³ occurred in the Tausamal microdistrict, killing four people and destroying homes. The landslide was triggered by a burst water pipe, causing local soil waterlogging (Fig. S4).^[30] On March 23, 2024, a second landslide with a volume of approximately 500 m³ occurred in Besagash, damaging homes and temporary structures after prolonged rainfall (Fig. S5).^[31]

Five of the seven landslides mentioned above occurred in the months of March, April, and May, when heavy rainfall occurs in the vicinity of the city of Almaty. One of these landslides (in 2023) occurred on February 27, at the very end of the month of February. The catastrophic landslide that occurred on February 8, 2024, was caused by the excessive moisture in the soil on the slope due to water from a nearby water pipe. In some years, the frozen upper parts of the slopes in this region begin to thaw in early February. It can also be assumed that the surface layer of the slope contained moisture stored by the pre-winter precipitation that fell in October and November of last year.

Based on the above analysis of landslides, it can be concluded that almost all of them occurred due to severe waterlogging of the clay soils on the slopes caused by heavy rainfall during the spring seasons.

4. Atmospheric precipitations

As is known,^[32] atmospheric precipitation plays an important role in the equilibrium and dynamics of the evolution of the

ecosystem, flora and fauna of the Earth as a whole and in its individual regions. The Kok Tobe mountain has its own unique climatic and geographical features.^[33] As the above analysis of landslides that took place in the mountain slopes located near the city of Almaty showed, atmospheric precipitation has a strong influence on the equilibrium of the slopes.

The following is an analysis of precipitation in the vicinity of Kok Tobe Mountain over the past twenty-five years, from 2000 to 2024. The precipitation information is obtained from the website^[34] of the National Hydrometeorological Service of the Republic of Kazakhstan.

Fig. 1 shows a histogram of total annual precipitation. As expected, the total precipitation is significantly unevenly

distributed over the years. For example, the maximum precipitation of 1,021 mm/year occurred in 2016, while the minimum precipitation of 489 mm/year occurred in 2021. In other words, 2.09 times more precipitation was recorded in 2016 compared to 2021. The average annual precipitation was 682 mm/year.

In Fig. 2, the histogram shows that more than half (52%) of the total annual precipitation falls within the range of 560 mm/year to 720 mm/year. Additionally, 46% of the precipitation in this range (24% of the total annual precipitation) falls within the narrower range of 600 mm/year to 640 mm/year, and 85% of the total annual precipitation is less than 660 mm/year (Fig. 3).

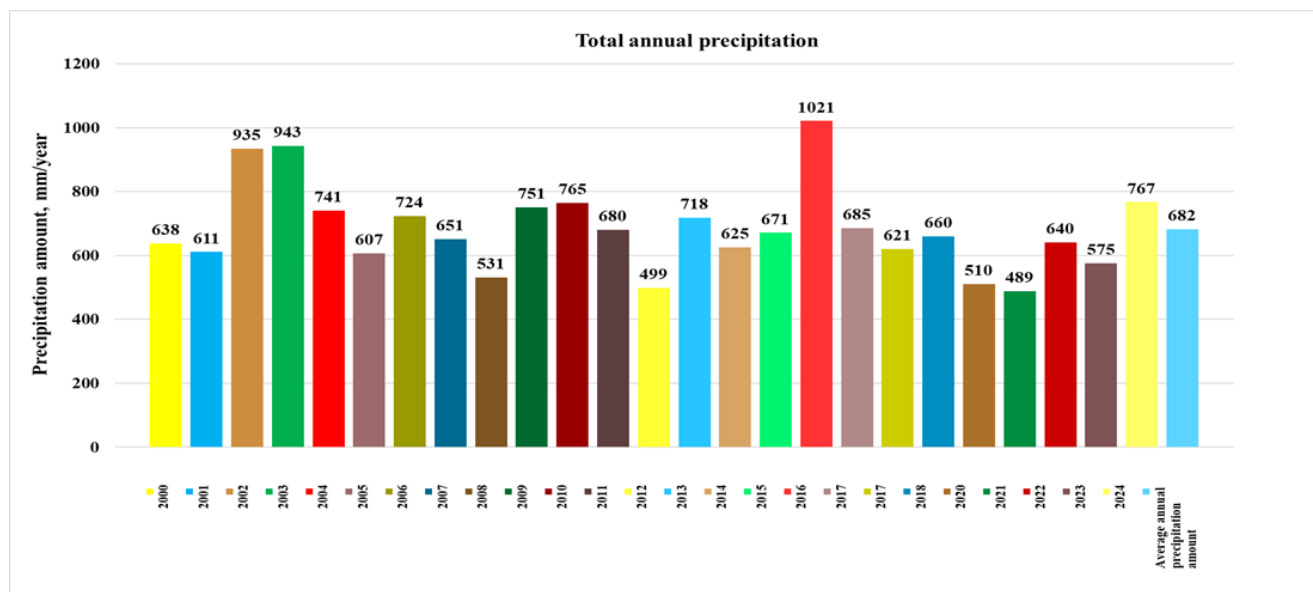


Fig. 1: Histogram of total annual precipitation.

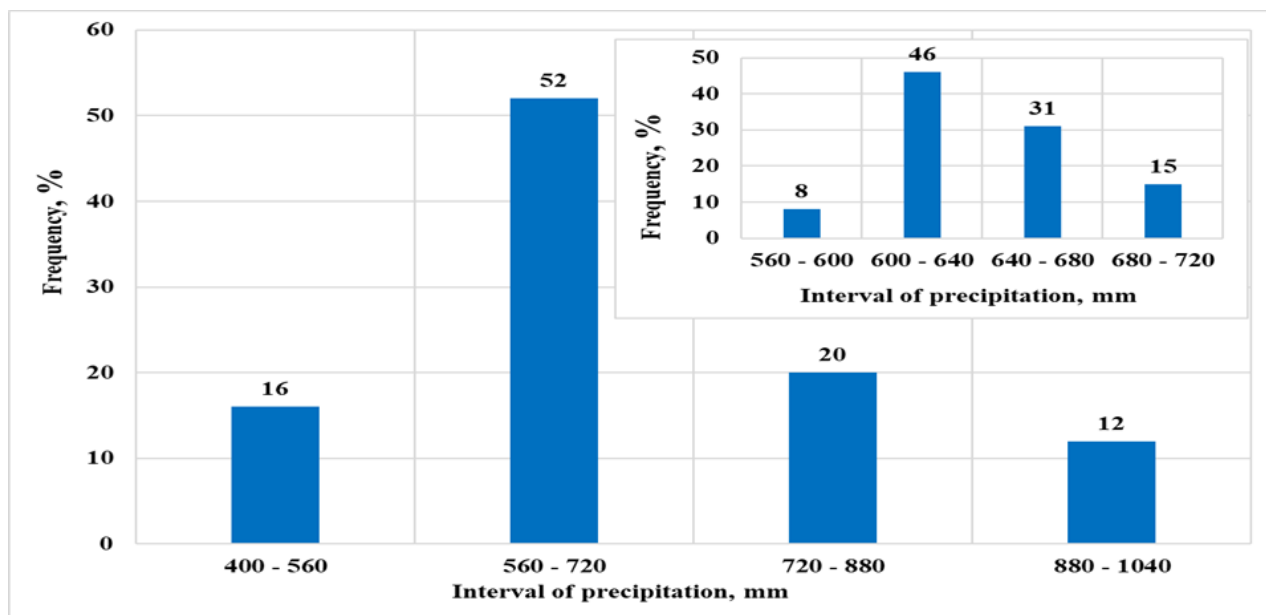


Fig. 2: Distribution of total annual precipitation.

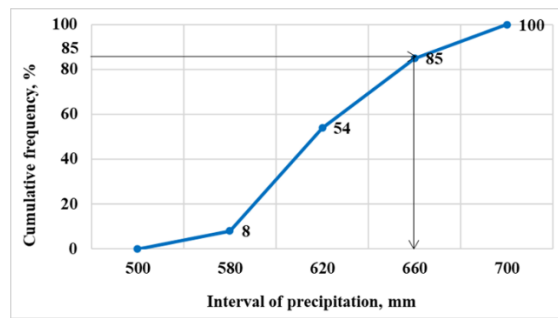


Fig. 3: Cumulative curve of total annual precipitation.

The histogram of monthly precipitation in different years is shown in Fig. 4. Fig. 5 shows the histogram of the maximum, minimum, and average monthly precipitation values from 2000 to 2024. From these histograms, it can be seen that the highest amounts of precipitation are typically observed in March, April, and May, while the lowest amounts are observed in January, February, August, and September. At the same time, the maximum monthly precipitation amount of 214 mm/month (which is one-third of the long-term average value of total annual precipitation) occurred in May. The average monthly precipitation amounts in March, April, and May were 82, 111,

and 97 mm/month, respectively.

The results of statistical processing (Fig. 6 and 7) show that three-quarters (74.34%) of monthly precipitation values were less than 72 mm/month, and a third of all monthly precipitation falls within the narrower interval of 48 mm/month to 72 mm/month. Almost a quarter (23.77%) of monthly precipitation from the interval of 0 to 72 mm/month falls within the even narrower interval of 24 mm/month to 36 mm/month. At the same time, 85% of all monthly precipitation is less than 54 mm/month.

The above factual information allows us to conclude that

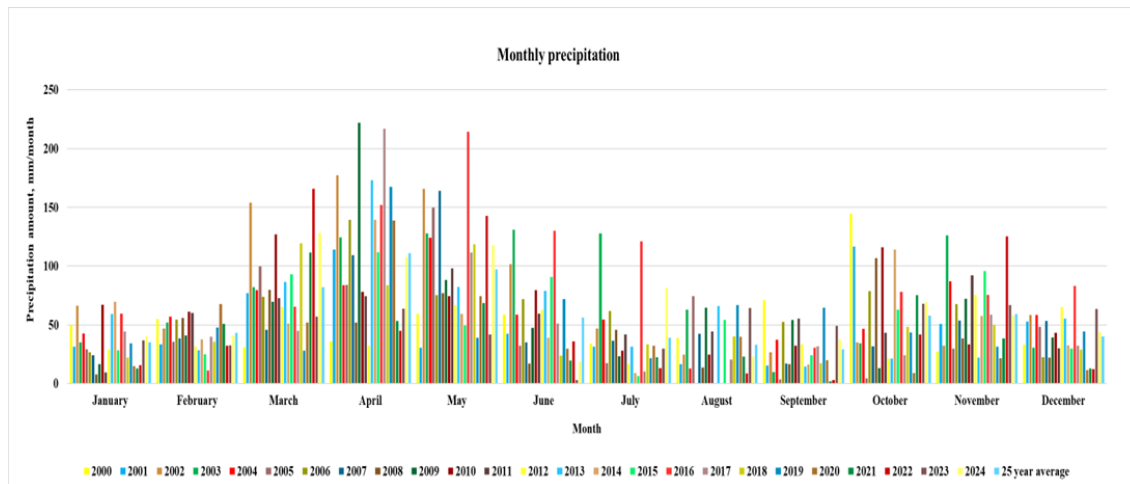


Fig. 4: Histogram of monthly precipitation in different years.

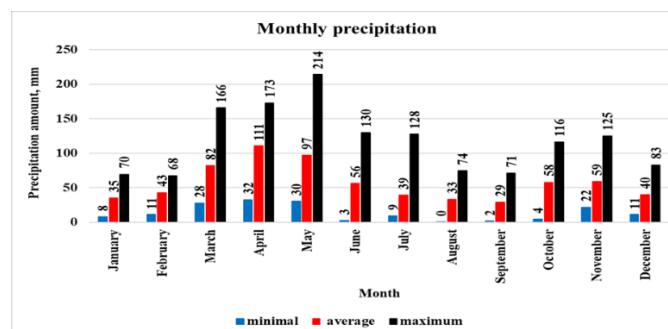


Fig. 5: Histogram of maximum, minimum, and average monthly precipitation values in different years.

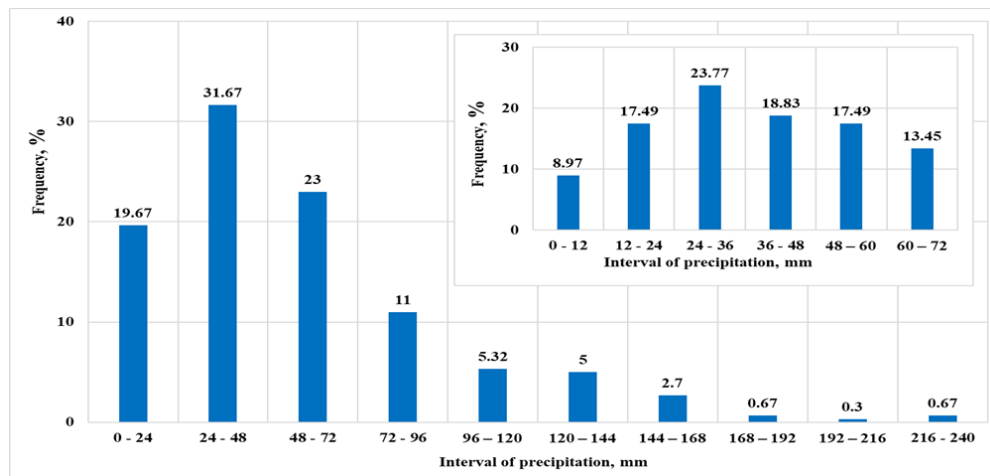


Fig. 6: Distribution of monthly precipitation.

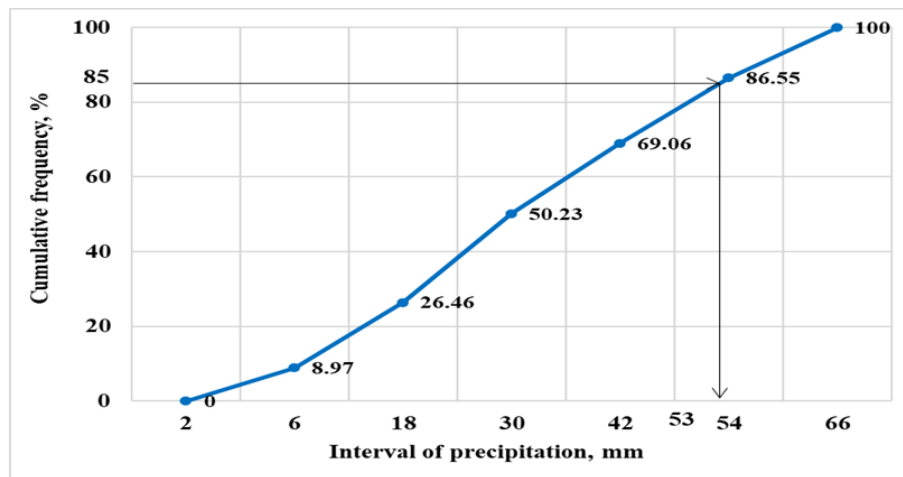


Fig. 7: Cumulative monthly precipitation curve.

due to the higher amount of precipitation in spring (rainfall and meltwater), the upper part of slopes composed of clay soils may become heavily saturated, which can lead to landslides.

5. Surface layer of the slope

The surface layer of a clay-based slope is periodically exposed to moisture from precipitation, especially in areas with high rainfall. The precipitation analysis carried out above showed that in the vicinity of Kok Tobe Mountain in the spring period (the months of March, April and May), in some years, heavy precipitation falls (up to 214 mm/month) after the thawing of snow and ice (after the winter period). Some of these sediments seep into the surface soil layer of the slope. It is known that the strength of clay soils decreases with increasing moisture content, which can lead to a loss of slope stability.

In works,^[35-37] it was established that after prolonged rains (up to 20 days), the upper part of the soil mass (clay soils, including loam) with a thickness of 60-70 cm becomes moist. Within this layer of clay soil, the moisture content varies from

30% (on the surface) to 26% (at a depth of 60-70 cm).

In this work, the following distribution of moisture is adopted by the thickness of the surface layer of the soil (loam) of the slope: thickness $h_1 = 0-10$ cm, moisture $W_1 = 30\%$; $h_2 = 10-50$ cm, $W_2 = 28\%$; $h_3 = 50-70$ cm, $W_3 = 26\%$. The rest of the soil slope has approximately the same moisture value equal to 12%. At this moisture content, loam has the following characteristics: specific cohesion $c = 35.0$ kPa, angle of internal friction $\varphi = 29.0$ degrees, specific gravity $\gamma = 21.0$ kN/m³. The values of specific cohesion c and angle of internal friction φ of loam at moisture contents of 26%, 28%, and 30% were determined based on the results of experimental studies by the authors of.^[38]

The specific gravity values of loam at different moisture levels are calculated using the following Eq. (1):

$$\gamma_w = \gamma_0 + \gamma_{\text{water}} \cdot W, \tag{1}$$

where γ_w – specific gravity of the soil at moisture content W (in fractions of unity);

γ_{water} – the specific gravity of water is 9.81 kN/m³;

γ_0 – specific gravity of dry soil (W=0).

The specific weight of dry soil (loam) is determined by the expression Eq. (2):

$$\gamma_0 = \gamma_{12} - \gamma_{\text{water}} \cdot 0.12 \quad (2)$$

where γ_{12} is the specific weight of the soil (loam) in its natural state (W=12%), which is equal to 21.0 kN/m³.

The characteristics of the slope soil (loam) at different moisture levels are given in Table 1.

Table 1: Characteristics of loam at different moisture levels.

Moisture W, %	Cohesion c, kPa	Angle of internal friction ϕ , degree	Specific gravity γ , kN/m ³
0	-	-	19.8
12	35.0	29.0	21.0
26	2.7	11.3	22.4
28	2.2	10.4	22.6
30	1.8	9.5	22.8

In further calculations of the stability of the Kok Tobe mountain slope using the classical and modified CCSS methods, in cases where the moisture content of the surface layer of the slope is taken into account, the real heterogeneous soil blocks are assumed to be homogeneous with averaged characteristics. The averaged values of the soil characteristics in the blocks are calculated using the following expressions Eq. (3)-(5):

$$c = \frac{\sum_{i=1}^m c_i \cdot h_i}{\sum_{i=1}^m h_i} \quad (3)$$

$$\phi = \frac{\sum_{i=1}^m \phi_i \cdot h_i}{\sum_{i=1}^m h_i} \quad (4)$$

$$\gamma = \frac{\sum_{i=1}^m \gamma_i \cdot h_i}{\sum_{i=1}^m h_i} \quad (5)$$

where h_i – thickness of layer i in the soil block;
 c_i, ϕ_i, γ_i – the specific cohesion, internal friction angle, and specific gravity of the soil in layer i .

6. CCSS methods

6.1 The classical CCSS method

One of the most common methods used to assess the stability of slopes of artificial structures (roads and railways, dams, earth dams, and others)^[39] and natural mountain slopes^[40] is the circular cylindrical sliding surface (CCSS) method. This is an engineering method that allows for a reliable assessment of the stability of slopes and embankments in many cases.

In this work, the CCSS method was used to obtain primary information about the stability of the northern slope of Kok Tobe Mountain, near which the section of the Greater Almaty

Ring Road (BACR) is located.

As is known, in the CCSS method, it is assumed that the loss of slope stability (slope) occurs by shifting the overlying soil mass along a circular cylindrical surface. The slope stability characteristic is adopted by the stability factor F_{Si} calculated by the Eq. (6):

$$F_{Si} = \frac{\sum_{i=1}^n M_{HF_i}}{\sum_{i=1}^n M_{SF_i}} = \frac{\sum_{i=1}^n (Q_i \cdot \cos \alpha_i \cdot \text{tg} \phi) \cdot R + c \cdot L \cdot R}{\sum_{i=1}^n (Q_i \cdot \sin \alpha_i) \cdot R} \quad (6)$$

where M_{HF} - moment of the holding force, kN·m;

M_{SF} - shear force moment, kN·m;

ϕ - angle of internal friction of the soil, degree;

c - specific soil cohesion, kPa;

L - sliding surface length, m;

R - sliding surface radius, m;

$S = Q \cdot \cos \alpha$ - shear force, kN;

$T = Q \cdot \sin \alpha$ - holding force, kN;

n - number of soil prisms.

The length of the sliding surface is determined by the Eq. (7):

$$L = 2 \cdot \pi \cdot R \cdot \frac{\alpha'}{360^\circ} \quad (7)$$

A slope is considered stable if the minimum stability factor F_S is greater than 1.3.^[41]

Slope stability calculations using the CCSS method are performed in the following sequence:

1. A series of estimated sliding surfaces is conducted under the slope below the horizontal ground surface.
2. The soil mass above the proposed sliding surface is divided into several vertical blocks (sections).
3. The entire, shear, and holding forces are determined for each block.
4. The moments of the shear and holding forces are calculated relative to the sliding centers.

5. For each proposed sliding surface, the stability factor F_S is determined as the ratio of the sum of moments of the holding forces to the sum of moments of the shear forces.

Apparently, the most difficult issue in the CCSS method is that the sliding centers are not known in advance. Because of this, it is necessary to choose a considerable number of assumed sliding surfaces with corresponding sliding centers.

The application of the Fellénus method^[2] significantly reduces the amount of calculations. The Fellénus method assumes that the centers of the sliding surfaces with the minimum values of the stability factor F_S lie on a straight line related to the geometric characteristics of the slope.

In this article, the classical CCSS method will be combined with the Fellénus method to assess a mountain slope composed of clay soil.

6.2 Modified CCSS method

In the work,^[40] a modified CCSS method was proposed and applied to assess the stability of a mountain slope. In this modified method, as in the classical CCSS method, the main assumption that the slope loses stability along a circular cylindrical sliding surface with radius R and sliding center O was retained. It was also assumed that the centers of the sliding

surfaces lie on the Fellenius straight line.

Since each proposed sliding surface is a part of a circle, it is characterized by the following three parameters: x_0 , y_0 , and R, which are the horizontal and vertical coordinates of the sliding center and the radius of the sliding surface, respectively (Fig. 8).

The parameters of the sliding surface are determined by the

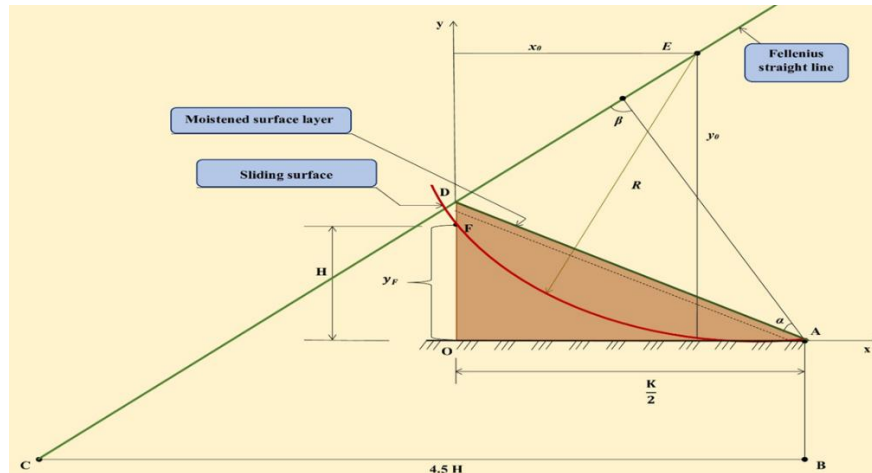


Fig. 8: Scheme of the modified CCSS method.

following expressions Eq. (8)-(10):^[43]

$$x_0 = \frac{\frac{K^2}{4} - y_F^2 + 2y_F a}{K - 2y_F b} \quad (8)$$

$$y_0 = a + b \cdot x_0 \quad (9)$$

$$R = \sqrt{\left(\frac{K}{2} - x_0\right)^2 + y_0^2} \quad (10)$$

The modified CCSS method can be called graph-analytical. Its graphical part includes a scaled drawing of the slope, its division into blocks, determination of the position of the Fellenius straight line and the assumed sliding surfaces; the analytical part consists of approximating the Fellenius straight line, calculating the parameter (x_0 , y_0 , R) of the sliding surfaces, the shear and holding forces in the blocks, the moments of these forces, and the FS stability factors.

The ability to determine the parameters of the sliding surfaces (x_0 , y_0 , R) significantly improves the accuracy and reduces the complexity of the CCSS method. For example, by knowing the values of the parameters x_0 , y_0 , and R, the sliding surfaces can be described analytically using the circle equation, and all subsequent calculations can be performed automatically.

It should be noted that the proposed modified CCSS method has a significant advantage over the finite element

method (FEM). So in FEM it is necessary to discretize the entire calculation domain into finite elements and in order to increase the accuracy of calculations it is necessary to increase the order of the polynomials approximating the displacement field in these finite elements, and significantly increase the number of finite elements, which leads to a significant increase in the number of calculations and time required. The proposed modified CCSS method eliminates this drawback. Calculations using it can be performed very quickly in standard Excel.

7. Results and discussion

7.1 Slope stability

In this work, the stability of the selected slope of Mount Kok Tobe is assessed under the following three conditions: condition 1 - the soil of the slope is homogeneous and is completely in its natural state; condition 2 - the surface layer of the slope 70 cm thick is moistened by rainwater and it is assumed that the sliding surfaces are deep (below the base of the slope); condition 3 - the surface layer 70 cm thick is moistened by rainwater and it is assumed that the sliding surfaces are close to the moistened surface layer of the slope.

The slope under consideration is divided into 26 blocks (Fig. 9). The stability factors of the slope in states 1 and 2 are determined by the classical CCSS method, and in state 3 – by the modified CCSS method.

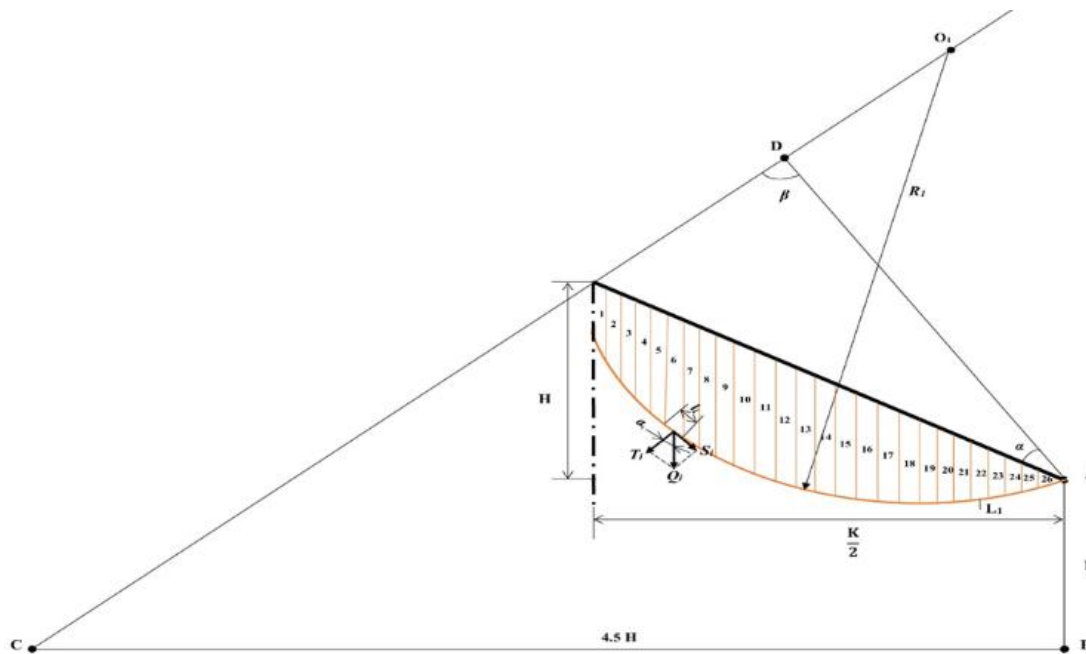


Fig. 9: Scheme for calculating slope stability using the CCSS method.

Table 2: Results of slope stability calculations (condition 1).

Sliding center	Radius, m	Sliding surface length, m	Sum of shear forces, kN	Sum of holding forces, kN	Stability factor F_s
O_1	354	414	183550	446997	1.43
O_2	363	422	118916	304594	1.54
O_3	375	431	87158	227813	1.62
O_4	390	402	58304	179368	1.94
O_5	402	379	52771	121655	1.52

Table 3: Results of slope stability calculations (condition 2).

Sliding center	Radius, m	Sliding surface length, m	Sum of shear force, kN	Sum of holding forces, kN	Stability factor F_s
O_1	354	414	183705	447380	1.41
O_2	363	422	119129	305269	1.51
O_3	375	431	87343	228159	1.57
O_4	390	402	58448	179731	1.87
O_5	402	379	42593	124874	1.86

Table 4: Results of slope stability calculations (condition 3).

Sliding center	Radius, m	Sliding surface length, m	Sum of shear force, kN	Sum of holding forces, kN	Stability factor F_s
O_6	345	409	171175	413380	1.4
O_7	342	406	179390	488218	1.57
O_8	339	402	192875	498001	1.48
O_9	339	390	219657	575523	1.5

The results of slope stability calculations under the above three conditions are presented in Tables 2-4.

As can be seen in Tables 2 and 3, in Fig. 10, the stability factors of the slope in states 1 and 2 are almost identical and range from 1.41 to 1.94. In other words, the moisture content of the upper layer of the slope due to rainwater has almost no effect

on the stability of the slope. This is likely due to the fact that the thickness of the moistened soil layer (70 cm) is much smaller than the vertical dimensions of the slope blocks.

The values of the slope stability factor in condition 3 are 1.4-1.57 (Fig. 11), which are approximately equal to the values of the stability factor in conditions 1 and 2 for sliding radii

ranging from 354 m to 375 m. It can also be said that the slope is not expected to lose stability when its surface layer is 70 cm thick and is moistened by rainwater.

It should be noted that the stability factors for sliding radii of 390 m and 402 m are slightly higher than those for smaller radii in all three conditions. This suggests that sliding surfaces with smaller radii may be more prone to instability.

The values of the slope stability factor in condition 3 are 1.4-1.57 (Fig. 11), which are approximately equal to the values of the stability factor in conditions 1 and 2 for sliding radii ranging from 354 m to 375 m. It can also be said that the slope is not expected to lose stability when its surface layer is 70 cm thick and is moistened by rainwater.

It should be noted that the stability factors for sliding radii of 390 m and 402 m are slightly higher than those for smaller radii in all three conditions. This suggests that sliding surfaces with smaller radii may be more prone to instability.

In general, for all three conditions, it can be observed that the stability factors range from 1.4 to 1.62 for sliding radii between 339 m and 375 m, which is slightly higher than the acceptable value of 1.3.

7.2 Local stability factors

Fig. 12 shows a histogram that displays the values of the local stability factors (f_s) determined for each of the 26 blocks (sliding radius of 354 m, condition 1) into which the slope under consideration was divided. As can be seen, the values of the local stability factors of the individual blocks vary greatly. Thus, in blocks from the first to the fifteenth, it gradually increases from 0.58 to 3.64. The most stable blocks are blocks 17, 18, and 25, with f_s values of 33.15, 33.57, and 49.56, respectively. Blocks 1-8 are not stable. It can be assumed that the stability of blocks 1-8 is ensured by the stability of other blocks, especially blocks 17, 18, and 25.

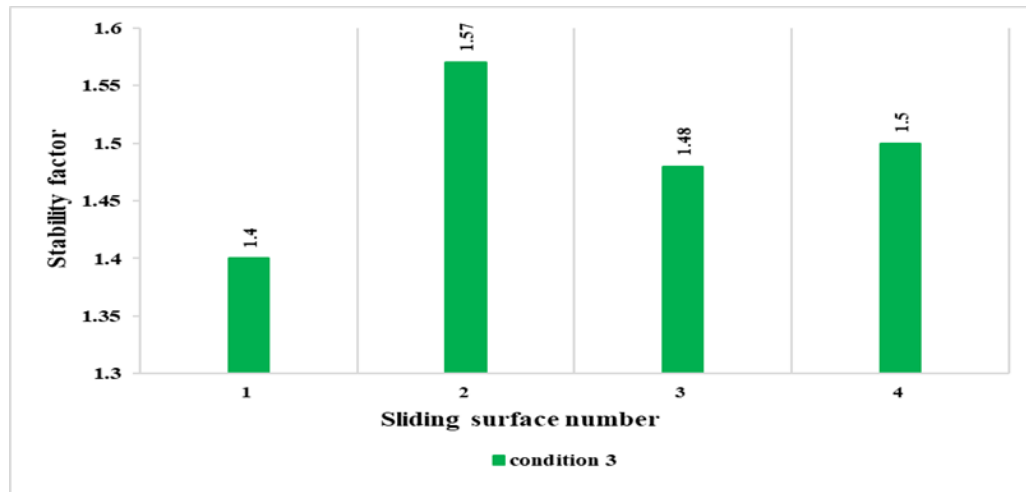


Fig. 10: Slope stability factors.

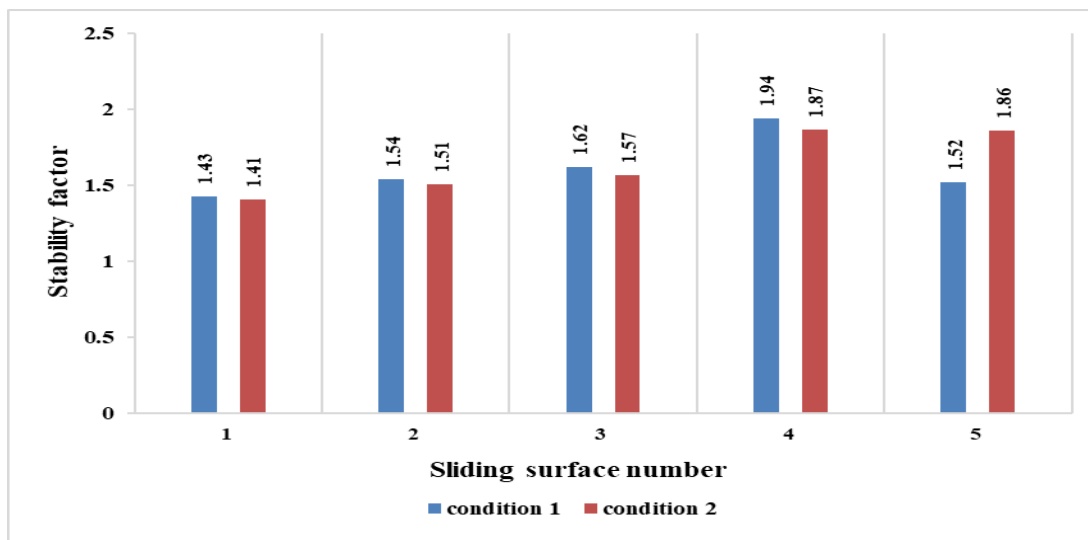


Fig. 11: Slope stability factors.

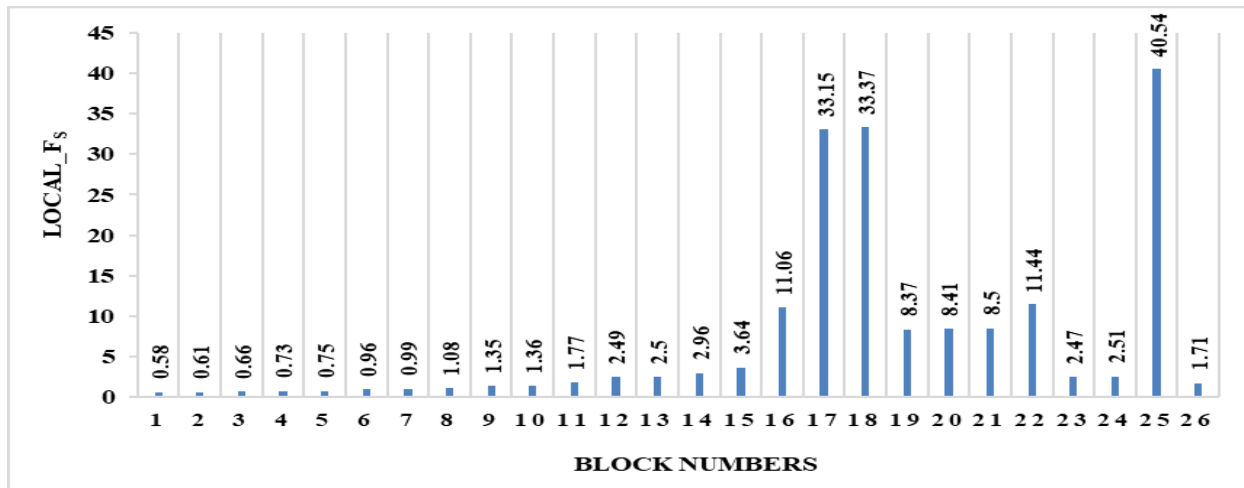


Fig. 12: Local slope stability factors.

Table 5: Values of soil characteristics at different moistures.

W, %	γ , kN/m ³	c, kPa	ϕ , degree
12	21	35	29
14	21.19	28.35	25.81
16	21.39	22.6	23
18	21.59	17.6	21.73
20	21.78	13	19.6

Table 6: Values of slope stability factor at different moistures.

Sliding center	Radius, m	Sliding length, m	surface	Stability factor F _s at moisture W, %				
				12	14	16	18	20
O ₁	354	414		1.43	1.24	1.1	1	1
O ₂	363	422		1.54	1.4	1.2	1.13	1
O ₃	375	431		1.62	1.4	1.22	1.22	1
O ₄	390	402		1.94	1.68	1.46	1.35	1.2
O ₅	402	379		1.52	1.32	1.14	1.04	1

7.3 Moisture effect on slope stability

To simultaneously evaluate the effect of moisture on slope stability and the sensitivity of the CCSS method to changes in soil characteristics, slope stability calculations were performed using the CCSS method at soil moisture contents of 14%, 16%, 18%, and 20%. The values of slope soil characteristics (c, ϕ , γ) at these moisture contents and at a moisture content of 12% (for comparison) are given in Table 5. The slope, as before, was divided into 26 blocks, each with the same dimensions (as at 12% moisture content). The calculation results are presented in Table 6.

As this table shows, soil moisture significantly affects slope stability. Even a small increase in moisture (by just 2%, from 12% to 14%) causes the slope to transition from a stable state (O₁: F_s=1.43) to an unstable state (O₁: F_s=1.24<1.3). As soil moisture continues to increase, all sliding surfaces

gradually become potentially susceptible. In other words, the probability of slope instability (landslide) rapidly increases.

Thus, we can conclude that:

- changes in soil characteristics due to changes in soil moisture greatly affect slope stability;
- the sensitivity of the CCSS method to changes in moisture content (soil characteristics) is high.

8. Recommendations

As it was established above, the factors of stability of the slope of Kok Tobe Mountain have insignificant reserves. And the values of the local stability factors in blocks 1-8 are unstable. These results force us to propose measures to ensure the stability of these parts of the slope.

There are several known ways to increase the stability of mountain slopes. They can be divided into engineering and

natural.^[42] Engineering methods include the installation of drains for draining surface and groundwater, strengthening slopes with retaining walls and terracing, as well as monitoring anthropogenic impacts. The natural method includes fixing the slopes using various local plants.

The aim is to increase the stability of the considered slope of Kok Tobe Mountain by sowing apple trees of the Aport variety on it. This variety traditionally grows at altitudes of 850-1250 m, which coincide with the conditions of Kok Tobe Mountain. It has a well-developed root system that grows at a significant rate (on average 240 cm or more), which makes it possible to increase the stability of mountain slopes in a short time.^[43] This recommendation can be implemented quickly and efficiently, as Kazakhstan is implementing a State program for 2024-2028, within which 11 stable aport clones have been selected.^[23] The sowing of aport species together with the grass cover (fescue, clover, tipchak) will increase the strengthening of the slope, reduce erosion and maintain the microclimate.

9. Conclusion

Over the past 10 years, 7 large landslides have occurred in the vicinity of Almaty, which was caused by severe waterlogging of clay soils of mountain slopes by heavy precipitation in the spring.

Over the past 25 years, an average annual precipitation of 600-720 mm/year has fallen near Kok Tobe Mountain. The maximum amount of precipitation (1,021 mm/year) occurred in 2016, and the minimum 489 mm/year in 2021. More than half (52%) of the total annual precipitation is in the range from 560 mm/year to 720 mm/year.

The greatest precipitation often falls in the months of March, April and May. The maximum monthly precipitation is 214 mm/month. The average rainfall in the months of March, April and May was 82, 111 and 97 mm/month.

The CCSS method is highly sensitive to changes in soil characteristics caused by changes in moisture content; CCSS calculations have shown that soil moisture content has a significant impact on slope stability.

A modified CCSS method has been developed, which increases accuracy and reduces the possibility of performing all calculations in an automated manner.

Moisture of the 70 cm thick surface layer by atmospheric precipitation has practically no effect on the stability of the slope of Kok Tobe Mountain.

To obtain information on the spatial distribution of slope stability, local stability factors for individual slope blocks were introduced, calculated, and analyzed. The calculation and analysis of local stability factors showed that the unstable part

of the slope is its upper part with a length of about 1/3 of the slope sequence. These features of the spatial heterogeneity of the stability of individual slope parts were taken into account when determining measures to improve its stability.

In general, the stability factors for sliding radii from 339 m to 375 m range from 1.4 to 1.62, which is slightly higher than the permissible values of 1.3.

It is proposed to increase the stability of the slope of Kok Tobe Mountain by sowing Aport apple trees on it, which grow at altitudes of 850 – 1250 m, coinciding with the conditions of Kok Tobe Mountain.

Acknowledgments

This research was supported by the Fundamental Research Grant from the Ministry of Science and Higher Education of the Republic of Kazakhstan (Grant Number: BR20280990, U. Joldasbekov IME).

Conflict of Interest

The authors declare no conflict interest.

Supporting Information

Applicable.

CRedit Statement

Bagdat Teltayev: Conceptualization, Methodology. **Bagdat Teltayev and Aizhan Muta:** Investigation. **Bagdat Teltayev and Aizhan Muta:** Writing - Original Draft Preparation. **Bagdat Teltayev, Aizhan Muta and Amandyk Tuleshov:** Writing - Review & Editing. **Bagdat Teltayev:** Supervision. All authors have read and agreed to the published version of the manuscript.

References

- [1] K. Terzaghi, *Theoretical Soil Mechanics*, New York, John Wiley & Sons, 1943, 1–526, doi: 10.1002/9780470172766.
- [2] W. Fellenius, Calculation of the stability of earth dams, *Transactions 2nd Congress on Large Dams*, Washington DC, 1936, 4, 445–459.
- [3] B. Khusanov, S. Normatov, O. Khaydarova, On one method for assessing the soil slopes stability, *AIP Conference Proceedings*, 2022, **2637**, 030012, doi: 10.1063/5.0119155.
- [4] M. Huang, C.-Q. Jia, Strength reduction FEM in stability analysis of soil slopes subjected to transient unsaturated seepage, *Computers and Geotechnics*, 2009, **36**, 93-101, doi: 10.1016/j.compgeo.2008.03.006.
- [5] Z. Su, L. Shao, A three-dimensional slope stability analysis method based on finite element method stress analysis, *Engineering Geology*, 2021, **280**, 105910, doi: 10.1016/j.enggeo.2020.105910.
- [6] R. P. Bhandary, A. Krishnamoorthy, A. U. Rao, Stability

- analysis of slopes using finite element method and genetic algorithm, *Geotechnical and Geological Engineering*, 2019, **37**, 1877-1889, doi: 10.1007/s10706-018-0730-5.
- [7] H. Jiang, Y.-X. Qiu, J.-J. Zhu, J.-T. Wang, C.-H. Zhang, X.-L. Du, A SEM-FEM-SPH framework for physics-based source-to-slope simulation of earthquake-induced landslides, *Engineering Geology*, 2025, **353**, 108127, doi: 10.1016/j.enggeo.2025.108127.
- [8] J. Zhang, X. Ma, M. Lu, A. Sharma, L. Zhang, Assessing highway resilience subjected to rainfall-induced slope failure, *Computers and Geotechnics*, 2025, **181**, 107134, doi: 10.1016/j.compgeo.2025.107134.
- [9] A. Timchenko, J.-L. Briaud, Stability of slope corners: a displacement-based FEM study, *Canadian Geotechnical Journal*, 2024, **61**, 562-574, doi: 10.1139/cgj-2022-0495.
- [10] W. He, T. Ishikawa, Y. Zhu, Wide/narrow-area slope stability analysis considering infiltration and runoff during heavy precipitation, *Soils and Foundations*, 2023, **63**, 101248, doi: 10.1016/j.sandf.2022.101248.
- [11] T. Ishikawa, T. Zhang, W. He, Y. Zhu, S. Kawamura, Role of road network for prevention and mitigation of runoff-induced geo-disaster under climate change, *Transportation Geotechnics*, 2024, **47**, 101283, doi: 10.1016/j.trgeo.2024.101283.
- [12] G. Ye, F. Zhang, A. Yashima, T. Sumi, T. Ikemura, Numerical analyses on progressive failure of slope due to heavy rain with 2d and 3d fem, *Soils and Foundations*, 2005, **45**, 1-15, doi: 10.3208/sandf.45.2_1.
- [13] L. Zhang, X. Jiang, R. Sun, C. Cui, H. Gu, Y. Qiu, A novel analytical approach for 3D stability of unsaturated soil slopes with cracks under rainfall infiltration, *Engineering Failure Analysis*, 2025, **175**, 109545, doi: 10.1016/j.engfailanal.2025.109545.
- [14] W. Gao, S. Ge, A comprehensive review of slope stability analysis based on artificial intelligence methods, *Expert Systems with Applications*, 2024, **239**, 122400, doi: 10.1016/j.eswa.2023.122400.
- [15] M. Mishra, V. R. Gunturi, T. F. Da Silva Miranda, Slope stability analysis using recent metaheuristic techniques: a comprehensive survey, *SN Applied Sciences*, 2019, **1**, 1674, doi: 10.1007/s42452-019-1707-6.
- [16] A. Rajabian, F. Vahedifard, D. Leshchinsky, A framework for analyzing the stability of geosynthetic reinforced soil walls under unsaturated conditions, *Journal of Geotechnical and Geoenvironmental Engineering*, 2024, **150**, 06024002, doi: 10.1061/jggef.kgteng-12069.
- [17] A. Rotaru, F. Bejan, D. Almohamad, Sustainable slope stability analysis: a critical study on methods, *Sustainability*, 2022, **14**, 8847, doi: 10.3390/su14148847.
- [18] R. K. Verma, P. Sharma, R. Singh, T. N. Singh, Evaluation of slope stability analysis using kinematic and chart method: a case study, *Journal of the Geological Society of India*, 2021, **97**, 1387-1395, doi: 10.1007/s12594-021-1877-x.
- [19] W. Alkasawneh, A. I. Husein Malkawi, J. H. Nusairat, N. Albataineh, A comparative study of various commercially available programs in slope stability analysis, *Computers and Geotechnics*, 2008, **35**, 428-435, doi: 10.1016/j.compgeo.2007.06.009.
- [20] D. A. Bouzid, Finite element analysis of slope stability by expanding the mobilized principal stress Mohr's circles-Development, encoding and validation, *Journal of Rock Mechanics and Geotechnical Engineering*, 2022, **14**, 1165-1179, doi: 10.1016/j.jrmge.2022.01.016.
- [21] A. V. R. Karthik, R. Manideep, J. T. Chavda, Sensitivity analysis of slope stability using finite element method, *Innovative Infrastructure Solutions*, 2022, **7**, 184, doi: 10.1007/s41062-022-00782-3.
- [22] Red Book of the Ile-Alatau National Park, Ile-Alatau National Park, <https://www.ile-alatau.kz/ru/redbook-ru/>.
- [23] Kazakh Government Unveils Program to Revive Legendary Aport Apple, The Astana Times, <https://astanatimes.com/2024/11/kazakh-government-unveils-program-to-revive-legendary-apor-apple/>.
- [24] Fire on Kok Tobe Extinguished in One and a Half Hours, Informburo, <https://informburo.kz/novosti/pozhar-na-kok-tobe-udalos-potushit-za-poltora-chasa>.
- [25] Landslide Destroyed a Cottage above Al-Farabi Avenue in Almaty, Tengrinews, <https://tengrinews.kz/events/almaty-opolzen-razrushil-kottedj-vyishe-prospekta-al-farabi-294180/>.
- [26] Landslide Came Down below Medeu High-Mountain Skating Rink, Almaty, Tengrinews, <https://tengrinews.kz/events/opolzen-soshel-v-almaty-nije-vyisokogornogo-katka-medeu-294860/>.
- [27] Landslide Came Down, Almaty, Tengrinews, <https://tengrinews.kz/events/opolzen-soshel-v-almaty-316080/>.
- [28] Landslide Came Down near Ajnabulak Sanatorium, Almaty, Tengrinews, <https://tengrinews.kz/events/v-rayone-sanatoriya-aynabulak-v-almaty-soshel-opolzen-317107/>.
- [29] Broken Windows and Cracks in Walls after Landslide, Almaty, Tengrinews, https://tengrinews.kz/kazakhstan_news/razbityie-okna-treschinyi-stenah-posledstviyah-opolznnya-bliz-492357/.
- [30] Main Cause of Landslide in Almaty Named by Kazselezaschita, Nur.kz, <https://www.nur.kz/incident/emergency/2059897-osnovnyu-prichinu-shoda-opolznnya-v-almaty-nazvala-kazselezaschita/>.
- [31] Soil Came Down in Almaty Region: There Is a Risk of Collapse of an Entire House, Sputnik Kazakhstan, <https://ru.sputnik.kz/20240323/grunt-soshel-v-almatinskoy-oblasti--est-risk-obrusheniya-tselogo-doma-43144501.html>.
- [32] N. Deguines, J. S. Brashares, L. R. Prugh, Precipitation alters interactions in a grassland ecological community, *Journal of Animal Ecology*, 2017, **86**, 262-272, doi: 10.1111/1365-2656.12614.
- [33] S. T. Ahmetova, K. I. Rodrigo, K. K. Duskaev, Analysis of atmospheric aridity in the territory of Almaty region under modern climate change conditions, *Bulletin of Kazakh National University. Series of Geography*, 2019, **54**(3), doi: 10.26577/JGEM.2020.v54.i3.06.
- [34] Kazhydromet – National Hydrometeorological Service of

Kazakhstan, Official Report, 2024.

[35] N. Klebanovich, Soil Hydrophysics, Minsk, 2016, 41.

[36] A. Naydenov, V. Vasilko, S. Terekhanova, Soil Moisture, (Principles and Ways of Regulating Soil Water Regime), KubSAU, Krasnodar, 2020.

[37] I. Kuznetsov, Tillage, Krasnodar, 1968.

[38] M. Dzhamanbaev, S. Omuraliev, Influence of moisture on the slope stability and strength properties of clay soil, *Problems of Modern Science and Education*, 2017.

[39] I. Gandelsman, Ground slope stability analysis, *E3S Web of Conferences*, 2023, **410**, 02016, doi: 10.1051/e3sconf/202341002016.

[40] B. B. Teltayev, A. N. Muta, Assessment of the stability of the slope of kok tobe mountain, *Engineered Science*, 2025, **35**, 1566, doi: 10.30919/es1566.

[41] U.S. Army Corps of Engineers (USACE), *Slope Stability. Engineer Manual EM 1110-2-1902*, US Army Corps of Engineers, Washington, DC, USA, 1993, https://www.publications.usace.army.mil/Portals/76/Publications/EngineerManuals/EM_1110-2-1902.pdf.

[42] C. Gong, D. Ni, Y. Liu, Y. Li, Q. Huang, Y. Tian, H. Zhang, Herbaceous vegetation in slope stabilization: a comparative review of mechanisms, advantages, and practical applications, *Sustainability*, 2024, **16**, 7620, doi: 10.3390/su16177620.

[43] PlantIDs Blog, How deep are the roots of an apple tree, <https://blog.plantids.com/how-deep-are-the-roots-of-an-apple-tree.html>.

Publisher's Note: Engineered Science Publisher remains neutral with regard to jurisdictional claims in published maps and institutional affiliations.

Open Access

This article is licensed under a Creative Commons Attribution 4.0 International License, which permits the use, sharing, adaptation, distribution and reproduction in any medium or format, as long as appropriate credit to the original author(s) and the source is given by providing a link to the Creative Commons license and changes need to be indicated if there are any. The images or other third-party material in this article are included in the article's Creative Commons license, unless indicated otherwise in a credit line to the material. If material is not included in the article's Creative Commons license and your intended use is not permitted by statutory regulation or exceeds the permitted use, you will need to obtain permission directly from the copyright holder. To view a copy of this license, visit <http://creativecommons.org/licenses/by/4.0/>.

©The Author(s) 2025.